Optimization of ANFIS-PID performance in bidirectional buck-boost DC-DC converter

Nor Farisha Diana Rosli* [iD], Wahyu Mulyo Utomo [iD], Afarulrazi Abubakar [iD], Suriana Salimin [iD], Tharnisha Sithananthan [iD]

Department of Electrical Engineering, Faculty of Electrical and Electronic Engineering, Universiti Tun Hussein Onn Malaysia.

Corresponding author: he220026@student.uthm.edu.my

Abstract:

This paper aims to investigate the performance of a bidirectional DC-DC converter utilizing an ANFIS-PID controller in closed-loop mode. This is because operating a bidirectional DC-DC converter in open-loop mode can result in several problems, including poor regulation, limited flexibility, and limited performance, especially in transient response and efficiency. Additionally, there is a risk of overloading the converter or damaging connected devices due to uncontrolled operation. Therefore, the main objective of this study is to address the critical requirement for enhanced response and load efficiency within the context of a three-phase interleaved bidirectional DC-DC converter designed for Hybrid Electric Vehicle (HEV) applications with 1 kW rated power of converter and 10 kHz switching frequency which exhibits 14.29% reduce overshoot in the system. This research aims to utilize the capabilities of an ANFIS-PID controller to optimize the dynamic responsiveness and load efficiency of the converter. The findings of the study reveal that the implementation of an ANFIS-PID controller leads to improved transient response and load efficiency, highlighting its potential to enhance bidirectional DC-DC converters. To design and simulate the behavior of the converter, MATLAB/Simulink software has been employed.

1. Introduction

The world is faced with the problem of fuel shortages because of rapid consumption and rising demand for oil, while the slower pace of finding new sources causes gasoline prices to rise. On the other hand, the burning of fossil fuels produces greenhouse gas emissions, which contribute to the harmful pollution of the atmosphere, particularly in heavily populated metropolitan areas. Furthermore, this process has contributed significantly to worldwide changes in both climatic patterns and the general ecosystem [1, 2]. Because of the demand for fuel economy, increasing environmental consciousness, and pollution-control measures, there is an urgent need to investigate eco-friendly transportation options that do not rely on fossil fuels so EV (electric vehicle) production was introduced because it is one of the ways to solve air pollution and fossil fuel issues.

This is because electric cars (EVs) generate ten times less CO_2 than conventional internal combustion engine vehicles (ICEVs), and their usage reduces CO_2 emissions in the transportation sector [3]. In EV, DC-DC converters primarily function as additional devices. DC-DC converters are designed to manage large amounts of electrical current. As a result, the inductor used in the converter tends to be bulky, which reduces the power density of the device. The size of the converter is influenced by the filter inductor, input, and output capacitors. In addition, due to the switching process involved, the DC-DC converter experiences significant fluctuations in input current. To overcome these challenges, interleaving or multi-phasing techniques are commonly used. The concept of an interleaved converter involves the integration of multiple power stages operating in parallel. In this setup, the input or source current is distributed across different phases, offering several advantages.

Firstly, it enhances the converter's power capacity, while also minimizing stress during switching operations. Additionally, it helps reduce the fluctuation in inductor currents, leading to improved overall heat distribution within the converter.

Half-bridge bidirectional buck-boost DC-DC converters are the most often used DC-DC converters for EVs because they are in high demand in wind, solar, and energy storage systems. As in a conventional buck-boost converter, it can manage the power flow in one direction, but differently in a bidirectional converter which can flow in both directions [4]. The converter is designed based on the input supply voltage and output voltage that is required in the system. Bidirectional DC-DC converters are devices designed to adjust voltage levels, allowing for both voltage increase (step-up) and voltage reduction (step-down). These converters possess the ability to transfer power in both the forward and reverse directions as needed. Fig. 1 shows the circuit of the bidirectional buck-boost DC-DC converter.

When have the converter, it is also possible to have the controller in the close-loop system. The main goal of a controller is to reduces the difference between the desired and actual values [5, 6]. Examples of controller that can be used are PID and ANFIS. This PID can be tuned to fulfill the performance specification and because of this, they are widely used due to their robustness and ease of implementation. The Ziegler-Nichols tuning method is commonly employed to regulate the parameters of a PID controller. This method aims to achieve rapid and satisfactory adjustments in controller gains and response while ANFIS is a tool that makes use of neural properties to comprehend the data set's logic and of fuzzy methodology to effectively apply that logic over the data set [7, 8].

In recent times, there have been numerous advancements in bidirectional DC-DC converter designs, involving a variety of controllers like the fuzzy logic controller. These controllers aim to minimize the steady-state error within the converter system [9]. Additionally, to mitigate fluctuations during a steady state, a sliding mode controller with fuzzy logic control has been introduced as one of the techniques [10]. To achieve a higher voltage gain and reduce output ripple, a novel approach involves the implementation of a
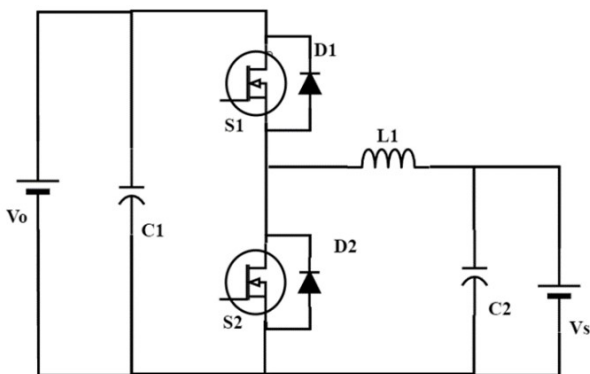
multiple-phase interleave bidirectional DC-DC converter. This converter utilizes closed-loop control to calculate a proportional-integral-derivative (PID) controller [11]. Furthermore, a hybrid controller, which combines two or more controllers within a single system, has been developed. For instance, the ANFIS-PID controller has been employed in a control arm rehabilitation device and can also be utilized in Electric Vehicles (EVs) to enhance the overall system response and achieve improved efficiency under both light and heavy load conditions [12, 13].

In this paper, multi-phase bidirectional DC-DC converters have been approached with ANFIS-PID controller support for the closed-loop system. This converter has used an interleaved technique in which the number of the converter consists of 2N controller switches in which N is the number of phases in the system [14]. The simulation and performance of the result of the ANFIS-PID will be compared with the PID result in terms of the system response. In section 1, along with the introduction, the basic of this project is discussed. Then operation and design of the bidirectional buck-boost converter are delineated in section 2. In section 3, the structure of the controller that will be used in this project is discussed. The simulation results of the comparison between ANFIS-PID and PID have been discussed in section 4 and followed by the conclusion in section 5.

2. Directional buck-boost converter

The purpose of interleaving is to reduce the size of the filtering component. The bidirectional DC-DC converter that is interleaved consists of three power modules connected in parallel, each operating with a phase shift equal to $360°$ divided by three. This parallel connection of power modules efficiently reduces undesirable low-frequency harmonics, resulting in reduced filtering stage size and cost [15]. In this circuit, the switch operates at $120°$, resulting in the inductor current being 120 degrees out of phase.

The overall current flowing through the inductor shows a slight fluctuation from peak to peak and operates at a frequency twice that of the individual inductor currents [14]. The incoming currents reach the filter C1 and the load, *Vo*. In a three-phase interleaved converter, the incoming current from the power source splits into three separate paths that run in parallel. As the three devices operate with a phase shift of 120 degrees, the resulting input current ripple is minimal. These interleaves can function in two modes, with the forward mode operating as a boost converter and the backward mode acting as a buck converter [16]. Fig. 2 shows a schematic diagram of the interleaved three-phase bidirectional buck boost DC-DC converter.

2.1 Forward mode (boost mode operation)

The three-phase interleaved DC-to-DC converter arrangement is formed in this operating condition by activating switches S2, S4, and S6 while switching off S1, S3, and S5. Diodes D2, D4, and D6 are reverse-biased during this phase, while diodes D1, D3, and D5 are forward-biased. During this time, the circuit runs in boost converter mode, with the inductor charging and the current traveling through inductors L1, L2, and L3 increasing linearly. When used in

Figure 1. Schematic diagram of bidirectional buck-boost DC-DC converter
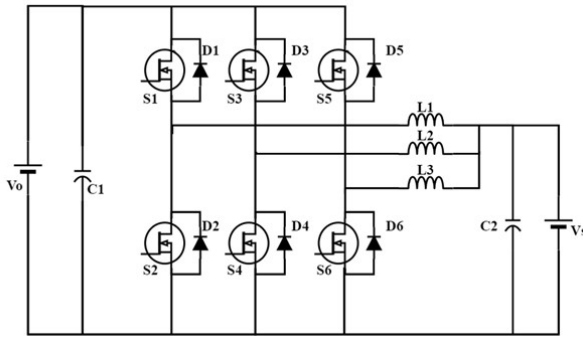
Figure 2. Schematic diagram of interleaved three-phase bidirectional buck-boost DC-DC converter.

electric car applications, this specific operational mode is referred to as the motoring mode.

2.2 Backward mode (buck mode operation)

When switches S1, S3, and S5 are enabled while switches S2, S4, and S6 are off, this mode often generates a buck for the interleaved DC-DC converter. D1, D3, and D5 are all reverse-biased, but D2, D4, and D6 are all forward-biased. The power flow from the load is reversed to charge the battery. The inductor current turns negative when the power flow is reversed. In EV applications, this mode is frequently called the regenerative braking function.

2.3 Converter design calculation

The output voltage in this circuit is obtained by this equation,

$$Vo = \frac{Vs}{(1-D)} \tag{1}$$

The inductor value and capacitor value can be calculated by this equation,

$$L = \frac{\Delta i_L^* f s}{D^* V s} \tag{2}$$

$$C = \frac{D^* Vo}{\Delta Vo^* R^* f s} \tag{3}$$

where Vo is the output voltage, Vs is the input voltage in this system, D is the duty cycle, fs is switching frequency, L is inductance, C is the capacitor, R is equivalent output resistance, Δi_L is the inductor ripple current and ΔVo is the output voltage ripple.

3. Structure of controller

3.1 PID controller

In this system, the PID controller is a type of discrete controller that operates in a discrete-time domain. These controllers are highly favored due to their simplicity of implementation and robustness. The PID controller continuously calculates an error value, which represents a non-identical between a desired setpoint and the measured process variable [17]. Based on this error, the controller computes and applies control actions to the system in order to minimize the error and achieve the desired output. The PID controller

consists of an error signal, which is used to generate proportional, integral, and derivative signals. These signals are then combined to create the plant feedback. The proportional part controls the system's response to the current error, the integral part adjusts the response based on the cumulative error, and the derivative part manages the response based on the rate of change of the error. The PID equation can be defined as follows.

$$u = kpe + kd\frac{de}{dt} + ki \int_0^t e(t) \tag{4}$$

In the context of this discussion, ki represents the integral parameter, kd stands for the derivative parameter, and kp signifies the proportional parameter of the PID controller. These PID controller parameters are typically fine-tuned using the Ziegler-Nichols tuning method, a technique known for fast and satisfactory gains and controller response [18]. However, the resulting coefficients are not optimal. To accurately determine the values of ki, kd, and kp, trial and error are employed for tuning the PID parameters.

3.2 ANFIS controller

After successfully training to model the inverse dynamics of the plant using the step input set point, ANFIS was able to calculate the requisite signal energizing the plant. The PID feedback controller is used in conjunction with the ANFIS controller to correct any residual tracking errors brought on by modelling errors and disturbances [17].
ANFIS is a combination of fuzzy logic controller (FLC) and Adaptive neuro network (ANN) that includes fuzzy rules and membership functions that have inverted input and output [19]. ANFIS has five stages before coming out with the true value. In this stage the input value has been sorted based on the rule which has been set as in the initial stages. Fig. 3 presents the ANFIS architecture that has been used in this project. The model contains 25 rules, two system inputs, the voltage error, e, and the delta error, de, and at the output the command f, so the first order Sugeno fuzzy inference with two inputs and 25 rules,
Rule 1: if x is A_1 and y us B_1 then $Z_1 = p_1x + q_1y + r_1$
Rule 2: if x is A_2 and y us B_2 then $Z_2 = p_2x + q_2y + r_2$
-

-

Rule n: if x is A_n and y us B_n then $Z_1 = p_nx + q_ny + r_n$
where, n is the number of the rules. From Fig. 3 the purpose of each layer can be defined as follows, Layer 1: this is the adaptive fuzzification layer. The membership function is from the bell function,

$$\mu_{Ai}(x) = \frac{1}{1 + \left[\frac{x - c_i}{a_i}\right]^{b_i}} \tag{5}$$

$$\mu_{Bi}(x) = \frac{1}{1 + \left[\frac{x - c_i}{a_i}\right]^{b_i}} \tag{6}$$

Here (a_i, b_i and c_i) is the parameter set as known as 'Premise Parameter'.
Layer 2: known as fuzzy rule layer, this layer points up the multiplication of all input signals, and every node is labeled as π the output of the product layer represents the following
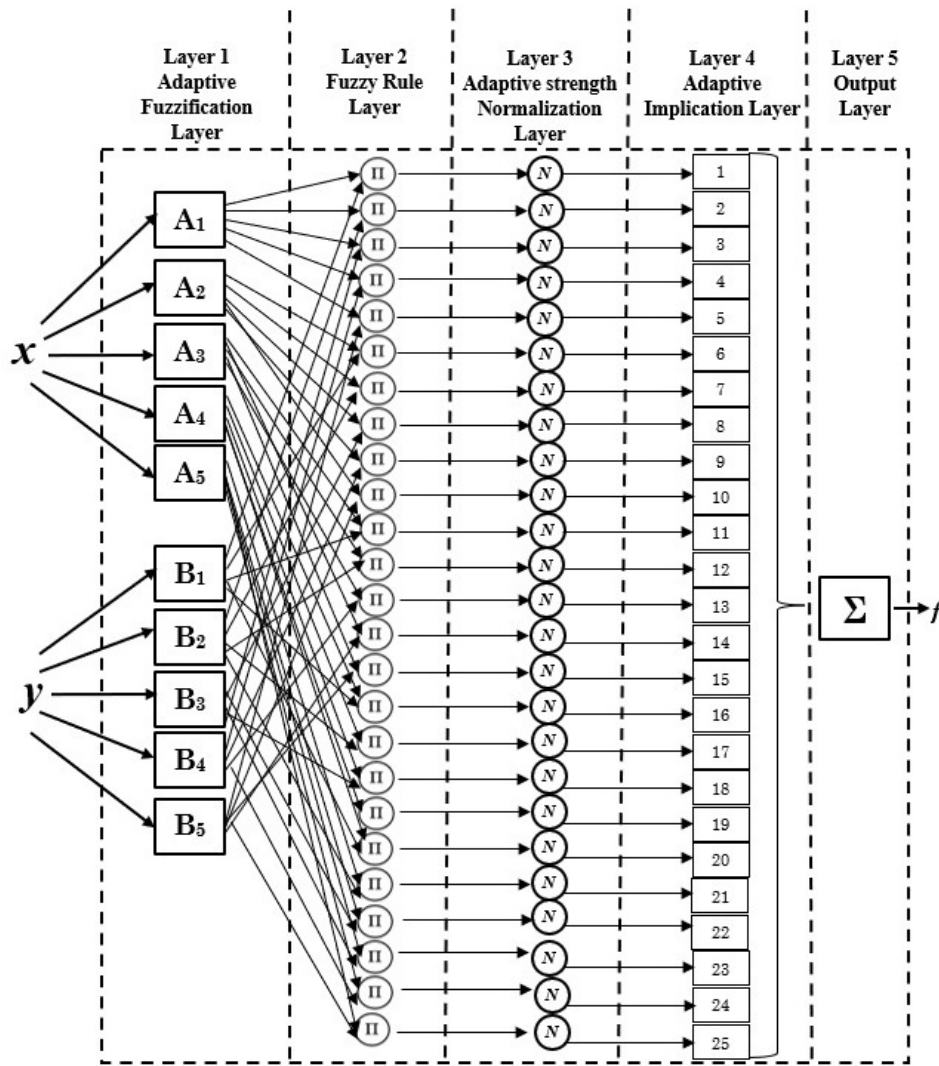
Figure 3. ANFIS Structure

node's input weight function. The expression of the output can be defined as below,

$$W_1 = O_{2,i} = \mu_{Ai}(x)x\mu_{Bi}(y) \quad \text{for} \quad i = 1,2 \tag{7}$$

$$W_2 = O_{2,j} = \mu_{Aj}(x)x\mu_{Bj}(y) \quad \text{for} \quad j = 1,2 \tag{8}$$

where the input layer is represented as W_1 and W_2 respectively.

Layer 3: this is normalization layer of the truth value of each rule. Firing strength shows how each rule is triggered, the active rule contributes to the system's final output. The expression of output in the normalization layer is given below,

$$W_1' = O_{3,i} = \frac{w_i}{w_1 + w_2} \quad \text{for} \quad i = 1,2 \tag{9}$$

$$W_2' = O_{3,j} = \frac{w_j}{w_1 + w_2} \quad \text{for} \quad j = 1,2$$

W_1' and W_2' represent the output of the normalized layer.

Layer 4: this system layer is critical because it performs an adaptive function that generates a membership function based on established fuzzy criteria. This function is critical

to the system, allowing it to make educated judgments and calculations based on input data.

$$W_1' f_i = O_{4,i} = W_i' x(p_i x + q_i y + r_i) \tag{10}$$

$$W_2' f_i = O_{4,j} = W_j' x(p_j x + q_j y + r_j) \tag{11}$$

Here W_i' and W_j' normalized strength that is obtained in layer 3 and $(p_i x + q_i y + r_i)$ and $(p_j x + q_j y + r_j)$ is a parameter set as known as 'Consequent Parameter'.

Layer 5: node has been labeled which denote the total of all sequence signals for the system that can be expressed as,

$$f = O_{5,i} = \Sigma W_i' f_i = \frac{\Sigma w_i f_i}{\Sigma w_i} \tag{12}$$

where the f represents the total output. The ANFIS model's optimization involves refining its two sets of parameters: the premises parameters and the consequences parameters. This optimization process is achieved through a hybrid learning method that combines the effectiveness of the gradient descent algorithm and the least squares estimation algorithm [17]. Table 1 shows the rule base used in this system. To tune the rule base in a fuzzy system, it is necessary to adjust

the fuzzy sets and membership functions associated with each input and output variable. Additionally, the rules themselves must be modified. This tuning process is necessary to guarantee that the fuzzy system accurately captures the dynamics of the underlying system and generates appropriate control actions. When it comes to tuning the rule base of a fuzzy system, there are a few different approaches that can be utilized, including manual tuning, automated tuning, and hybrid approaches. Overall, one of the most important steps in the process of developing an efficient fuzzy system is the tuning of the rule base. The specific application and the available resources are two factors that should guide the selection of the tuning method.

Table 1. Rule base for bidirectional DC-DC buck-boost converter.

c de	NB	NS	Z	PS	PB
NB	NB	NB	NL	NS	Z
NS	NB	NS	NS	Z	PS
Z	NB	NS	Z	PS	PB
PS	NS	Z	PS	PS	PB
PB	Z	PS	PB	PB	PB

The error input range is categorized using linguistic variables, including NB (negative big), NS (negative small), Z (zero), PS (positive small), and PB (positive big). Similarly, the delta error input range employs linguistic variables identical to those used for the error range. This linguistic variable-based approach is utilized to describe and characterize the input ranges for both error and delta errors, enhancing the system's precision and interpretability.

3.3 ANFIS-PID controller

One of the hybrid controllers is ANFIS-PID controller that has been developed by integrating two components which are the ANFIS controller and PID controller [20]. ANFIS-PID controller has been designed with fixed parameters to enhance its performance. The plant is indicating the converter model in the system. The ANFIS system was effectively trained to approximate the plant's inverse dynamics. The ANFIS controller contains fuzzy modules and membership functions with inverted input and output. To handle any remaining tracking errors caused by disturbances and modelling inaccuracies, a PID feedback controller is employed alongside the ANFIS control system [13]. The designation

of the block diagram of the ANFIS-PID is shown in Fig. 4. By combining fuzzy logic and PID control, ANFIS-PID can accurately track setpoints, enhancing performance when following desired trajectories or reference signals. Moreover, ANFIS-PID can enhance fault tolerance by adapting its control strategy when system faults or disturbances occur, increasing operational reliability.

3.4 PWM signal generator

The PWM signal generator is commonly utilized in various applications like power converters, audio amplifiers, and motor speed control because of its efficiency and precise power level control. When generating the PWM signal, the controller's input is determined by the voltage difference between the reference voltage and the actual output voltage of the controller. The output from the controller will generate the duty cycle signal before the PWM generator produces the PWM signal. The PWM generator will produce six pulse PWM signals according to the duty cycle from the output controller. The PWM signal pattern for the three-stage bidirectional DC-DC converter is illustrated in Table 2.

Table 2. The basic pattern of the PWM signal in the control switch.

Stages	Mosfet (ON)	Mosfet (OFF)
1		S_1,S_2,S_3,S_4,S_5,S_6
2	S_1	S_2,S_3,S_4,S_5,S_6
3	S_3	S_1,S_2,S_4,S_5,S_6
4	S_5	S_1,S_2,S_3,S_4,S_6
5	S_1,S_3	S_2,S_4,S_5,S_6
6	S_1, S_5	S_2,S_3,S_4,S_6
7	S_3,S_5	S_1,S_2,S_4,S_6

4. Simulation result

Before we started using the ANFIS controller to test our new bidirectional buck-boost converters, we built the entire system in MATLAB/Simulink. This allowed us to use S-functions for custom coding, and we used typical Simulink blocks for the rest of the components. This setup was crucial for evaluating our controllers effectively.

The bidirectional buck-boost converter was constructed using an interleaved method. Its purpose was to produce a stable 85 V output from a 48 V input voltage, making it well-suited for applications involving integrated circuits em-
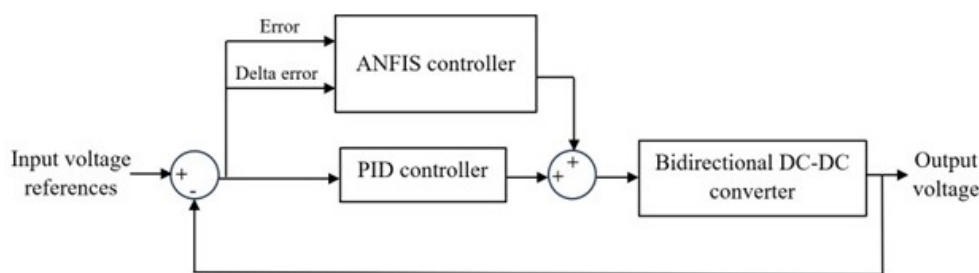

Figure 4. Purpose block diagram of ANFIS-PID control system.

bedded within a system. The power stage components were configured to switch at a frequency of 10 kHz. Detailed system specifications can be found in Table 3.

Table 3. Specification simulation parameter

Components	Part name	Rating values
Vs	Input voltage	48 V
Vo	Output voltage	100 V
$L_1L_2L_3$	Inductances	1000 μH
C_1C_2	Capacitances	4000 μF
f_s	Switching frequency	10 kHz
R	Resistance	15 Ω
P_o	Rated power	1 kW

The Simulink platform was employed to incorporate the discrete PID controller, while the coefficients for the controller were determined by applying the Ziegler-Nichols method. The calculated values for the coefficients were observed to be $Kp = 0.0249$, $Ki = 0.256$, and $Kd = 0.001$.

The ANFIS was specifically designed to accommodate two designated inputs: "error" and "change in error." Its output was configured to determine the necessary alteration in switching duty. Each input was further subdivided into five constants, which functioned as the output membership functions. This resulted in a total of 25 rules ($5 \times 5 = 25$) within the system. To train the ANFIS, data from the open-loop response of the planned bidirectional buck-boost converter was utilized. As depicted in Fig. 5, a proposed model of the three-phase interleaved bidirectional buck-boost converter, integrated with ANFIS and PID control, was connected in parallel to the converter for experimentation and analysis.

The designed system's transient and steady-state performance was thoroughly examined for its intended purpose. Additionally, a PID-based bidirectional buck-boost converter was implemented to draw a comparison with the outcomes achieved by the hybrid controller. The transient simulation result can be seen in Fig. 6.

After analyzing the responses generated by the controller, several parameters were recorded to evaluate the performance of the hybrid system. The measurements of these parameters can be observed in Table 4.

The ANFIS-PID controller shows improve of 3% in terms

of overshoot which high overshoot can lead to instability in the system response.

Table 5 and Table 6 show the results of when the load has been changing. As can be seen from both tables, the overshoot increases as the load increases which leads to changes in the output voltage. For load 18 Ω and 25 Ω, in both tables does not have any changes in the overshoot which is in stable stated value for the circuit but the rise time for both loads in ANFIS-PID and PID has slightly changed which around 2 s to 5 s.

Table 4. Performance of the simulated controller.

Parameter	PID	ANFIS-PID
Rise time, ms	16.65	17.99
Overshoot, V	100.8	98.41
Overshoot, %	17.29	14.29
Settling time, s	0.36	0.30

Table 7 shows the output voltage in different inputs and different loads. For the input voltage at 60 V, the output for ANFIS-PID and PID remains the same as the circuit reaches the stable limit but when the input voltage is lower than 60 V, the output voltage for ANFIS-PID in every load is lower than the PID output voltage. While Table 8 shows overshoot for different loads at different input voltages.

The overshoot of the ANFIS-PID in every single load at different input voltages is lower than PID which is good for the system as it is more stable, while when overshoot is high, it can lead to instability of the system as shown in Fig. 7.

Table 9 shows the rise time in this system. For ANFIS-PID, the rise time is a little bit slower than PID around 0.001 s until 0.005 s depending on the load use. The lower rise time is at 12 Ω load of PID and the higher rise time is ANFIS-PID at 18 Ω load. Fig. 8 shows the graph of the rise time and input voltage in different loads.

Settling time for input 60 V, was the fast steady-stated compared to the others. The lower settling time is from 12 Ω at 10 V of input voltage which takes around 1.836 s to achieve the table stated. As seen in Table 10, the ANFIS-PID is a fast timer in achieving a stable state compared to the PID controller. Although it can be said that this controller does not hold so much improvement, this ANFIS-PID controller can lead to stability and can control the quality of the system.
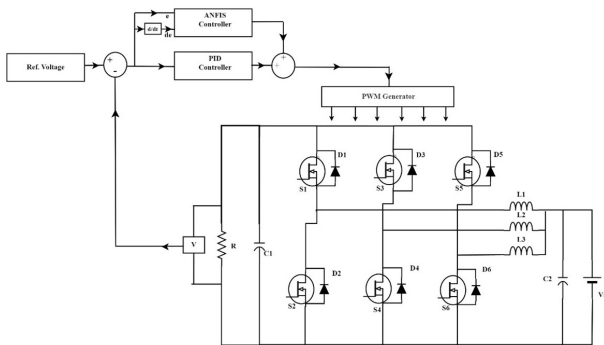

Figure 5. Proposed model of the three-phase interleaved bidirectional buck-boost converter with the proposed controller.
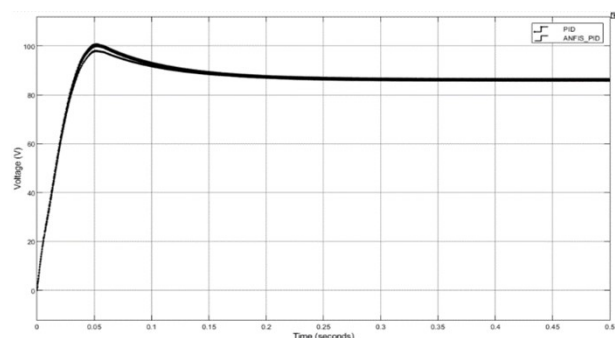

Figure 6. Output voltage of the ANFIS-PID and PID

Table 5. Performance of the simulated ANFIS-PID with different load.

Load(Ω)	Rise time, ms	Overshoot, V	Overshoot, %	Settling time, s
10	24.99	140.7	144.95	0.36
12	9.33	118.10	71.21	0.36
15	16.65	100.8	17.29	0.36
18	82.25	103.5	0.58	0.36
25	34.00	142.3	0.42	0.36

Table 6. Performance of the simulated PID with different load.

Load (Ω)	Rise time, ms	Overshoot, V	Overshoot, %	Settling time, s
10	24.32	137.70	139.73	0.30
12	10.67	115.20	67.00	0.30
15	17.99	98.41	14.29	0.30
18	84.48	103.5	0.58	0.30
25	39.00	142.30	0.42	0.30

Table 7. Input voltage vs output voltage in different loads.

Vs (V)	12 Ω		15 Ω		18 Ω	
	ANFIS-PID (V)	PID (V)	ANFIS-PID (V)	PID (V)	ANFIS-PID (V)	PID (V)
10	79.80	96.78	71.87	97.22	72.13	99.78
20	72.14	99.25	72.27	100.2	72.05	100.3
30	71.83	99.83	71.65	99.89	64.40	100.20
40	71.63	99.39	71.70	95.98	85.87	85.87
50	71.85	93.10	89.63	89.63	107.30	107.30
60	86.22	86.22	107.60	107.60	128.80	128.80

Table 8. Input voltage vs overshoot in different loads.

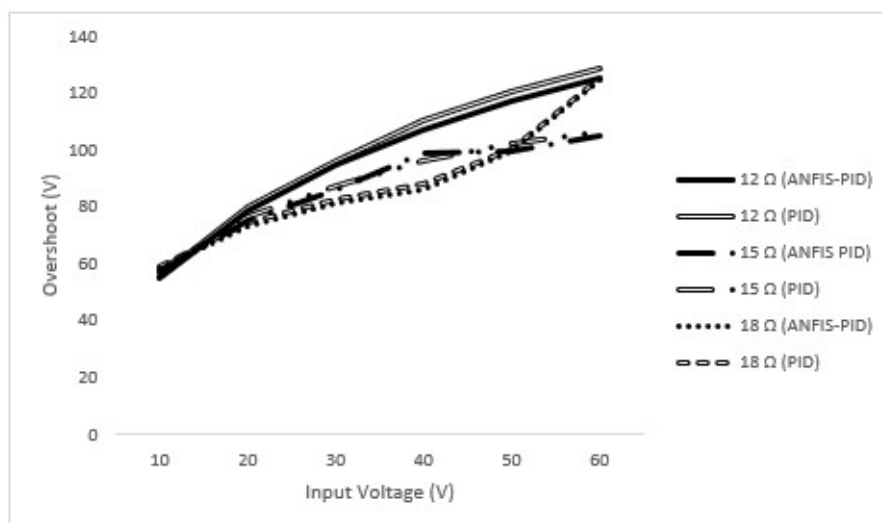| Vs (V)	12 Ω		15 Ω		18 Ω	
	ANFIS-PID (V)	PID (V)	ANFIS-PID (V)	PID (V)	ANFIS-PID (V)	PID (V)
10	54.89	55.66	56.49	57.70	58.35	59.08
20	78.23	79.84	74.85	76.35	72.88	74.24
30	94.44	95.95	85.82	87.32	81.00	82.50
40	107.10	109.90	98.88	95.66	86.00	87.66
50	117.00	120.00	99.35	101.90	99.36	99.97
60	125.30	128.50	104.70	106.40	124.60	125.30

Figure 7. Graph of the input voltage vs overshoot in different loads.

Table 9. Input voltage vs rise time in different loads.

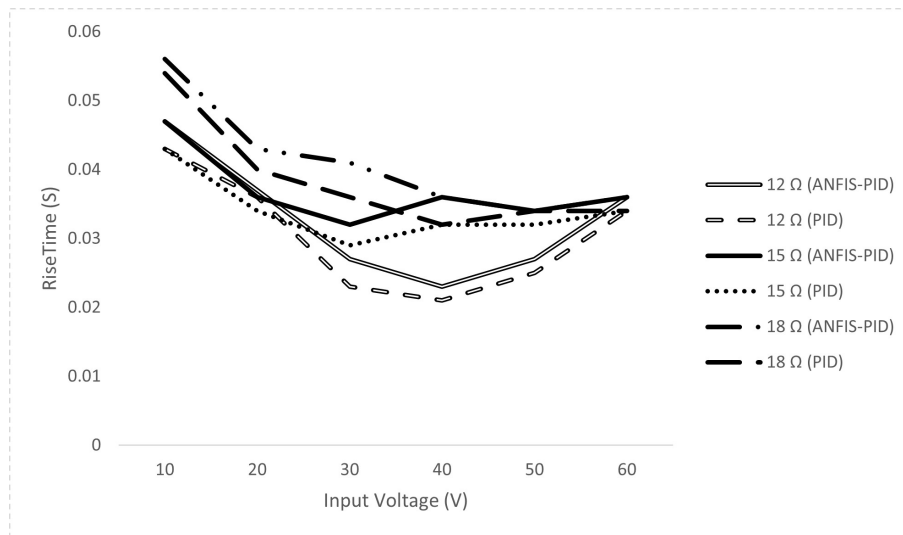| Vs (V)	12 Ω		15 Ω		18 Ω	
	ANFIS-PID (s)	PID (s)	ANFIS-PID (s)	PID (s)	ANFIS-PID (s)	PID (s)
10	0.047	0.043	0.047	0.043	0.056	0.054
20	0.037	0.036	0.036	0.034	0.043	0.040
30	0.027	0.023	0.032	0.029	0.041	0.036
40	0.023	0.021	0.036	0.032	0.036	0.032
50	0.027	0.025	0.034	0.032	0.034	0.034
60	0.036	0.034	0.036	0.034	0.036	0.034

Figure 8. Graph of the input voltage vs rise time in different loads.

Table 10. Input voltage vs settling time in different loads

Vs (V)	12 Ω		15 Ω		18 Ω	
	ANFIS-PID (s)	PID (s)	ANFIS-PID (s)	PID (s)	ANFIS-PID (s)	PID (s)
10	1.378	1.836	1.197	1.434	1.109	0.954
20	1.245	1.028	1.129	1.068	1.094	1.013
30	1.264	1.094	1.251	0.956	1.192	0.956
40	1.251	1.166	0.36	0.30	0.142	1.107
50	0.083	0.150	0.279	1.107	0.567	0.567
60	0.305	0.375	0.205	0.246	0.205	0.246

5. Conclusion

This paper presented a design and simulation result of the product ANFIS-PID which is in hybrid controller categories connected with interleaved bidirectional buck-boost DC-DC converter. This hybrid system has the capability to harness both the advantages of the PID and ANFIS controllers in terms of performance and power efficiency. The controller and converter have been simulated using MATLAB/Simulink, employing the S-function API.

The primary objective of this study is to achieve improved response dynamics and increased load efficiency in the bidirectional buck-boost controller. The simulation results demonstrate that both approaches yield the desired output. However, the ANFIS-PID controller approach outperformed the PID controller approach in terms of maximum overshoot in the circuit. Hence, these controllers efficiently manage disturbances within the system, consequently enhancing the overall performance and efficiency of the buck-boost converter.

Authors Contributions

All the authors have participated sufficiently in the intellectual content, conception and design of this work or the analysis and interpretation of the data (when applicable), as well as the writing of the manuscript.

Availability of data and materials

Data presented in the manuscript are available via request.

Conflict of Interests

The authors declare that they have no known competing financial interests or personal relationships that could have appeared to influence the work reported in this paper.

Open Access

This article is licensed under a Creative Commons Attribution 4.0 International License, which permits use, sharing, adaptation, distribution and reproduction in any medium or format, as long as you give appropriate credit to the original author(s) and the source, provide a link to the Creative Commons license, and indicate if changes were made. The images or other third party material in this article are included in the article's Creative Commons license, unless indicated otherwise in a credit line to the material. If material is not included in the article's Creative Commons license and your intended use is not permitted by statutory regulation or exceeds the permitted use, you will need to obtain permission directly from the OICCPress publisher. To view a copy of this license, visit https://creativecommons.org/licenses/by/4.0.

References

[1] G. Hill, O. Heidrich, F. Creutzig, and P. Blythe. "**The role of electric vehicles in near-term mitigation pathways and achieving the UK 's carbon budget**.". *Appl. Energy*, 251:pp. 113111, 2018.

[2] P. Wang, C. Zhao, Y. Zhang, J. Li, and Y. Gao. "**A bidirectional three-level DC-DC converter with a wide voltage conversion range for hybrid energy source electric vehicles**.". *J. Power Electron*, 17(2): pp. 334–345, 2017.

[3] S. Omer A. Dik and R. Boukhanouf. "**Electric vehicles: V2G for rapid, safe, and green EV penetration**. ". *Energies*, 15(803):pp. 2–27, 2022.

[4] J. Chen and B. Lin. "**Implementation of digital bidirectional buck- boost converter with changeable output voltage for electric vehicles**.". *IEEE International Future Energy Electronics Conference (IFEEC)*, :pp. 1–6, 2021.

[5] F. S. M. Alkhafaji, W. Z. W. Hasan, M. M. Isa, and N. Sulaiman. "**A novel method for tuning PID controller**.". *J. Telecommun. Electron. Comput. Eng*, 10 (1):pp. 33–38, 2018.

[6] E. Aircrafts, Á. Ojeda-rodríguez, P. González-vizuete, and J. Bernal-méndez. "**A survey on bidirectional dc/dc power converter topologies for the future hybrid and all electric aircrafts**.". *Energies*, 13(18), 2020.

[7] M. Bharathidasan, V. Indragandhi, and B. Aljafari. "**Hybrid controlled multi-input dc/dc converter for electric vehicle application**.". *Int. Trans. Electr. Energy Syst*, 2023, 2023.

[8] S. Ghosh. "**Neuro-fuzzy-based IoT assisted power monitoring system for smart grid**.". *IEEE Access*, 9: pp. 168587–599, 2021.

[9] K. Bendaoud et al. "**Implementation of fuzzy logic controller (FLC) for DC-DC boost converter using Matlab/Simulink**.". *Journal of Sensors and Sensor Networks. Special Issue: Smart Cities Using a Wireless Sensor Networks*, :pp. 1–5, 2017.

[10] K. Mumtha, V. Mahalakshmi, and S. Usha Devi. "**Proposed fuzzy logic controller for Buck DC-DC converter**.". *Int. J. Fuzzy Syst. Adv. Appl*, 7:pp. 24–28, 2021.

[11] F. Wang, B. Su Y. Wang, and C. Teng. "**Three-phase interleaved high step-up bidirectional DC-DC converter**.". *IET Power Electron*, 13(12):pp. 2638–2650, 2020.

[12] M. H. Jali, N. E. S. Mustafa, T. A. Izzuddin, R. Ghazali, and H. I. Jaafar. "**ANFIS-PID controller for arm rehabilitation device**.". *Int. J. Eng. Technol*, 7(5):pp. 1589–1597, 2015.

[13] U. A. Shaikh, M. K. AlGhamdi, and H. A. AlZaher. "**Novel product ANFIS-PID hybrid controller for buck converters**.". *J. Eng*, 2018(8):pp. 730–734, 2018.

[14] C. Lai, Y. Lin, and D. Lee. "**Study and implementation of a two-phase interleaved bidirectional dc/dc converter for vehicle and dc-microgrid systems**.". *Energies*, 8(9):pp. 9969–9991,, 2015.

[15] R. Kumar, P. K. Behera, and M. Pattnaik. "**A comparative analysis of two-phase and three-phase interleaved bidirectional dc-dc converter**.". *IEEE Int. Students' Conf. Electr. Electron. Comput. Sci. SCEECS*, : pp. 1–5, 2023.

[16] S. Dusmez, S. Member, A. Hasanzadeh, and A. Khaligh. "**Comparative analysis of bidirectional thre -level DC-DC converter for automotive applications**.". *IEEE Trans. Ind. Electron*, , 2015.

[17] M. H. Almawlawe and I. Dahham. "**Controlling switched DC-DC converter using ANFIS in comparison with PID controller**.". *IOP Conference Series: Materials Science and Engineering*, , 2020.

[18] A. F. Algamluoli. "**Voltage controller of dc-dc buck boost converter with proposed PID controller**.". *Int. J. Adv. Res. Comput. Eng. Technol*, 9(1), 2020.

[19] R. Mechgoug, N. Tkouti, and F. Okba. "**A adaptive neuro-fuzzy inference system (ANFIS) controller for a 9-level inverter for grid-connected PV systems**.". *Neuro Quantology*, 21(6):pp. 1120–1134, 2023.

[20] T. S. Babu. "**A comprehensive review of hybrid energy storage systems: converter topologies, control strategies and future prospects**.". *IEEE Access*, 8, 2020.